

# Realistic time-lags and litter dynamics alter predictions of plant–soil feedback across generations

Suzanne X. Ou<sup>1</sup>, Gaurav S. Kandlikar<sup>2, 3</sup>, Magdalena L. Warren<sup>1</sup>, and Po-Ju Ke<sup>4, †</sup>

<sup>1</sup>Department of Biology, Stanford University, Stanford, CA 94305, USA

<sup>2</sup>Department of Biological Sciences, Louisiana State University, Baton Rouge, LA 70803, USA

<sup>3</sup>Division of Biological Sciences, University of Missouri, Columbia, MO 65211, USA

<sup>4</sup>Institute of Ecology and Evolutionary Biology, National Taiwan University, Taipei, Taiwan

January 25, 2024

## **ORCID information:**

Suzanne Xianran Ou: 0000-0002-8542-4149

Gaurav S. Kandlikar: 0000-0003-3043-6780

Magdalena L. Warren: 0000-0003-0115-5066

Po-Ju Ke: 0000-0002-8371-7984

**Total word count for main body of text:** 5679

**Word count for each section:**

Introduction: 1036

Materials and Methods: 2535

Results: 848

Discussion: 1260

**Number of color figures:** 5

**Number of supporting information:**

Methods: 1

Figures: 3

---

† Correspondence author: [pojke@ntu.edu.tw](mailto:pojke@ntu.edu.tw)

## 1 **Summary**

- 2     • Plant–soil feedback is a critical process in natural plant communities. However, it remains  
3       unclear whether greenhouse-measured microbial effects manifest in natural systems with  
4       temporally separated growing seasons as classic experiments often overlook seasonal time  
5       lags and litter dynamics.
- 6     • We modified the classic two-phase experiment to study plant–soil feedback for three Cali-  
7       fornian annual plant species. Our response phase used soil inoculum obtained either im-  
8       mediately after plant conditioning, after a six-month dry period with the conditioning plant  
9       removed, or after a dry period with the litter of the conditioning plant. We characterized soil  
10      bacterial and fungal communities in different treatments and employed recent advancement  
11      in plant–soil feedback theory to predict plant coexistence.
- 12    • Temporal delays and the presence of litter caused distinct responses in the fungal and bacterial  
13      communities, resulting in divergent microbial compositions at the end of the response phases.  
14      The delayed response treatments also affected microbially mediated stabilization, fitness  
15      differences, and invasion growth rates differently across species pairs, influencing predictions  
16      of plant coexistence.
- 17    • Our study highlights that the interplay between seasonal delays and litter dynamics prevents  
18      the direct extrapolation of plant–soil feedback measurements across multiple seasons, em-  
19      phasizing the necessity of considering natural history when predicting microbially mediated  
20      plant coexistence.

## 21 **Keywords**

22 Annual plants, Invasion growth rate, Litter decomposition, Microbial community, Modern coexis-  
23 tence theory, Natural history, Seasonality

## 24 Introduction

25 The interactions between plants and soil microbes have gained increasing recognition as a pivotal  
26 force in shaping plant communities (Bever *et al.*, 2010, van der Putten *et al.*, 2013). The effects of  
27 these interactions on plant community dynamics are most commonly studied under the plant–soil  
28 feedback (PSF) framework, which captures the effects of bidirectional interactions in which plants  
29 simultaneously alter and are affected by the soil microbial community (Bever *et al.*, 1997). To  
30 implement this framework in empirical studies, PSF is often quantified through two-phase experi-  
31 ments that separate the feedback process into distinct "conditioning" and "response" phases (Bever  
32 *et al.*, 1997, 2012). Plant performances during the response phase are measured to predict how  
33 soil microbes influence plant coexistence (Crawford *et al.*, 2019, Yan *et al.*, 2022). However, despite  
34 a vast body of literature showing that soil microbes can exert strong controls over plant species  
35 coexistence, connecting the predictions from such two-phase studies to the observed dynamics of  
36 plant communities in nature remains challenging (Forero *et al.*, 2019, Beals *et al.*, 2020, Beckman  
37 *et al.*, 2022, Png *et al.*, 2023). A promising approach for addressing this challenge is to adopt the  
38 classic two-phase design to better reflect the natural conditions under which PSF arises in the field  
39 (Gundale & Kardol, 2021).

40 Greenhouse experiments of plant–soil feedback typically simplify the temporal dynamics of  
41 feedback by conducting the conditioning and response phases sequentially, without any temporal  
42 separation between them. While this design likely captures the effects of microbial feedback among  
43 plants growing concurrently, whether these same effects manifest in communities characterized  
44 by temporally separated plant growing seasons or in communities where time-lags occur between  
45 soil conditioning and its subsequent recolonization is less clear. For example, Esch & Kobe (2021)  
46 found that in a temperate hardwood forest, *Prunus serotina* adults cultivate a soil community that  
47 suppresses the growth of conspecific seedlings, but this suppressive effect erodes within months  
48 of plant death. Thus, the long-term consequences of soil conditioning are unclear if there are time  
49 lags between adult death and subsequent arrival/growth of seedlings in the conditioned soils,  
50 which is especially likely in plant communities characterized by dispersal and/or seed limitation  
51 (Ehrlén & Eriksson, 2000). Similarly, in systems where plant dynamics are highly seasonal, the  
52 conditioning effects that build up during one growing season may not translate directly to affect

53 plants in subsequent growing seasons if the soil community is reshaped during the intervening  
54 period (Barnard *et al.*, 2013). Such dynamics are likely to be especially relevant in Mediterranean-  
55 type annual plant communities frequently used in PSF experiments (e.g., Bonanomi *et al.*, 2012,  
56 Siefert *et al.*, 2019, Kandlikar *et al.*, 2021), where winter growing seasons are punctuated by dry  
57 summers of plant senescence (Elmendorf & Harrison, 2009). Furthermore, recent theoretical  
58 studies have demonstrated that the temporal dynamics of plant–soil feedbacks can substantially  
59 alter predictions of microbially mediated plant coexistence (Ke & Levine, 2021, Miller & Allesina,  
60 2021). Thus, both empirical and theoretical evidence suggests that incorporating the natural  
61 temporal dynamics of plant communities into studies of plant–soil feedback might enable more  
62 robust predictions of how soil microbes shape plant coexistence in nature.

63 Another aspect of the soil conditioning process that is largely overlooked in two-phase plant–  
64 soil feedback experiments is that, in nature, the soil microbial community is shaped not only by the  
65 active conditioning effects of plants as they grow but also by the dead tissue (i.e., litter) that plants  
66 deposit onto the soil. Specifically, recent literature has shown that plant litter of different species  
67 can influence microbial communities by introducing phyllosphere microbes to the soil (Whitaker  
68 *et al.*, 2017, Fanin *et al.*, 2021, Minás *et al.*, 2021) and by releasing chemicals and nutrients that  
69 affect soil microbial community assembly (Veen *et al.*, 2021). These litter-induced changes in the  
70 microbial community can subsequently result in different plant–soil feedback on the responding  
71 plants (Veen *et al.*, 2019, Aldorfová *et al.*, 2022). For example, in systems with distinct phenology or  
72 seasonality, using soil collected at the end of the growing season rather than after decomposition  
73 would fail to capture the full impact of litter dynamics. Despite the role of litter dynamics in  
74 shaping soil communities in all systems, this process is largely overlooked in plant–soil feedback  
75 experiments, which typically remove all plant material at the conclusion of the conditioning phase.  
76 Incorporating the role of litter in plant–soil feedback is thus an important step for bridging the gap  
77 between classic experiments and natural conditions.

78 To better predict the long-term consequences of plant–soil feedback in natural systems, we  
79 also need theoretically robust metrics to extrapolate greenhouse experimental results. The original  
80 theory of plant–soil feedback popularized a pairwise feedback metric that quantifies how soil mi-  
81 crobes drive frequency-dependent stabilization (e.g., via host-specific pathogens; Bever *et al.*, 1997,

82 Eppinga *et al.*, 2018). Recent theoretical advances have integrated plant–soil microbe interactions  
83 with modern coexistence theory (Kandlikar *et al.*, 2019, Ke & Wan, 2020), which utilizes invasion  
84 growth rates to predict species coexistence (i.e., quantifying whether each plant can establish in its  
85 competitor’s monoculture equilibrium from low density; Turelli, 1978, Chesson, 2000). Specifically,  
86 plant coexistence requires the stabilizing effects of microbes to overcome microbially mediated fit-  
87 ness differences, with the former capturing how microbes benefit both plants by driving negative  
88 frequency dependence while the latter capturing how microbes disproportionately impact one  
89 plant species over the other (Kandlikar *et al.*, 2019, 2021, Yan *et al.*, 2022). Evaluating coexistence  
90 outcomes on the basis of species’ invasion growth rates can also yield important insights for eluci-  
91 dating the underlying interactions in experimental data (Grainger *et al.*, 2019, Ke & Wan, 2020, 2023).  
92 Examining the impact of experimental manipulation through these theoretical metrics enables a  
93 more nuanced understanding of the pathways through which plant–soil feedback influences plant  
94 coexistence.

95 Here, we conducted an experiment to address two questions about the role of soil microbes  
96 in shaping plant coexistence in annual grasslands: (1) How do seasonal time lags and plant lit-  
97 ter decomposition interact with the conditioning process to alter the soil microbial community?  
98 (2) How do these changes to the soil community scale up to impact the predicted consequences  
99 of plant–soil feedback? To address these questions, we modified the two-phase greenhouse ex-  
100 periment and conducted three fully factorial response treatments. These treatments used soil  
101 inoculum obtained either immediately after plant conditioning, after a six-month dry period time  
102 lag with the removal of the conditioning plant, or after a similar dry period with the litter of the  
103 conditioning plant left intact. We quantified the absolute abundance of soil bacterial and fungal  
104 communities at the end of the conditioning and response phases, enabling us to evaluate how the  
105 soil inocula from each response treatment triggered different microbial communities. We then  
106 employed modern coexistence theory to predict the consequences of plant–soil feedback based  
107 on microbially mediated stabilization, fitness difference, and invasion growth rates (Kandlikar  
108 *et al.*, 2019). Our results demonstrated that both time lag and plant litter altered the outcome of  
109 plant–soil feedback, with varying effects across species pairs. This work underscores the need to  
110 incorporate natural history when predicting microbially mediated plant coexistence.

## 111 **Methods**

### 112 **Study system**

113 We focused on three native Californian winter annual plants: a legume *Acmispon wrangelianus*  
114 (ACWR; Fabaceae), a grass *Festuca microstachys* (FEMI; Poaceae), and a forb *Plantago erecta* (PLER;  
115 Plantaginaceae). In spring 2019, we collected seeds from the University of California Sedgwick  
116 Reserve in Santa Barbara County, California, USA (34°41' N, 120°02' W), where all three species  
117 co-occur. In this Mediterranean-type climate, annual plants complete their life cycle and senesce  
118 in the hot, dry summer lasting about six months (May-October mean temperature = 18.9°C,  
119 mean monthly precipitation = 4.57 mm; data from 2014–2023). The new generation germinates  
120 following rain in the cool, wet winters (November-April mean temperature = 12.3°C, mean monthly  
121 precipitation = 54 mm). In September 2020, prior to winter rains, we collected field soil from  
122 Sedgwick Reserve to serve as microbial inoculum. To ensure that the field microbial community  
123 was not pre-conditioned by species in our experiment, we collected soil from four locations where  
124 there were no individuals of our focal species in a 1 m radius. The soils were kept at 4° and  
125 transported to the lab within 12 hours, where equal amounts of soil from each location were sifted  
126 through a 2 mm sieve and homogenized. Prior to the experiment setup, we subsampled the field  
127 soil and stored it at -80° for later DNA sequencing of the microbial community. One fraction of the  
128 field soil was then used to inoculate the conditioning phase pots, and the remainder was stored at  
129 0°C until further use in the response phases as a reference soil treatment.

### 130 **Greenhouse experiment and soil sampling**

131 We modified the classic two-phase experiment to study how seasonal time lag and plant litter  
132 affect the soil microbial community and plant competitive outcomes. Specifically, our growth  
133 chamber experiment consisted of three fully factorial response treatments, using soil inocula that  
134 went through different handling treatments to represent these natural history factors (Fig. 1). We  
135 collected soil samples at different stages of the experiment and characterized the microbial commu-  
136 nity by high-throughput sequencing. Plant competitive outcomes were predicted by measuring  
137 plant biomass performance at the end of the experiment.

138 *Conditioning phase*

139 To cultivate soil microbes associated with each species, we grew three high-density monocultures  
140 (8 g viable seed/m<sup>2</sup>) of each species in bleach-sterilized 1-gallon pots (Fig. 1). We first filled each pot  
141 with 2.60 L sterilized potting mix (equal parts sand, clay, peat, perlite, and vermiculite; autoclaved  
142 twice, each 2 hours with a 24-hour resting period in between). We then added 0.30 L of field soil to  
143 each pot and topped it with a 0.10 L layer of sterilized potting mix to achieve a 10% volume of live  
144 inoculum. Into each pot, we sowed 0.141 grams of seeds of a single species, which we had surface-  
145 sterilized by soaking in 1% bleach for 2 minutes and washing with ultrapure water twice for 1  
146 minute each. We stored pots at 4°C for five days to trigger germination, after which we moved pots  
147 to a growth chamber (25°C, 60% humidity, 10:14 hour day:night cycle) for 80 days, approximately  
148 the length of a complete growing season. In addition to the 9 large conditioning pots, we grew  
149 10 replicate individuals of each species in sterilized potting mix to serve as phytometers between  
150 the different phases of the experiment (3 species × 10 replicate individuals = 30 pots). We rotated  
151 control plants (30 pots) and conditioning monoculture pots (9 pots) weekly within the growth  
152 chamber.

153 The conditioning phase of the experiment concluded in December 2020. At this time, we  
154 randomly chose soil from one monoculture pot for each species to serve as the inoculum source  
155 for the "immediate" response treatment (green pots in Fig. 1). We designated the remaining two  
156 monoculture pots per species for the two time-lagged response treatments, and left these in the  
157 growth chamber (25°C, 10% humidity, 10:14 hour day:night cycle) for an extra six-month dry period  
158 to mimic the temporal gap between two consecutive seasons. From one of these, we removed all  
159 aboveground biomass of the conditioning plant (grey pot in Fig. 1), whereas in the other we left  
160 all plant tissue intact (brown pot in Fig. 1). Thus, for each species, we were able to evaluate  
161 the effects of soil conditioning on subsequent plant growth without any time lag ("immediate"  
162 treatment), and could also evaluate how the presence of litter interacts with time lags to affect  
163 the plant performance during the "delayed" response phase (Fig. 1). Before using the conditioned  
164 monoculture pots for their corresponding response phase, we collected soil samples from each pot  
165 to characterize how seasonal time lag and plant litter influenced the soil microbial community (see  
166 section *DNA sequencing of the microbial community*).



167 *Response phase*

168 To create soil inocula for the "immediate" response phase, we removed the aboveground biomass  
169 from one conditioning monoculture pot per species, and sifted the soil through a 2 mm sieve to  
170 remove roots and homogenize the soil. We autoclaved half of this soil to create the sterilized  
171 inocula; the other half served as the live inoculum. We grew 10 replicate individuals of each  
172 species with either live or sterilized inoculum from each of the three species' freshly conditioned  
173 monoculture pot (i.e., 3 plant species  $\times$  3 soil inoculum  $\times$  2 sterilization treatments  $\times$  10 replicates  
174 = 180 pots). These plants in immediate response treatment correspond to the typical experimental  
175 procedure in plant–soil feedback experiments, which use soil inoculum collected at the end of the  
176 conditioning phase. To quantify the impact of time lag and litter presence, we started another  
177 round of response phase (i.e., the two delayed treatments) in June 2021 using soil inoculum that  
178 experienced an additional six months of dry period after the conditioning phase, thereby more  
179 closely mimicking the natural temporal dynamics of these grasslands. For these treatments, we  
180 grew 10 replicates of each species with live and sterile inoculum from the corresponding "delayed"  
181 and "delayed with litter" monoculture pots of each of the three species (i.e., 3 plant species  $\times$  3 soil  
182 inoculum  $\times$  2 delay treatments  $\times$  2 sterilization treatments  $\times$  10 replicates = 360 individuals).

183 For the response phase pots, we filled 125 mL Deepots (Stuewe & Sons, Inc.) with sterilized  
184 potting mix and 10% volume of soil inoculum, and covered the inoculum with a thin layer of steril-  
185 ized potting mix. We surface-sterilized and pre-germinated seeds, and transplanted seedlings into  
186 the pots so that each pot had a single individual. As evaluating microbially mediated coexistence  
187 outcomes requires growing plants in a reference soil (*sensu* Kandlikar *et al.*, 2019), we also grew  
188 10 replicate individuals of each species using unconditioned field soil as inoculum (previously  
189 collected and stored at 0°C; blue pots in Fig. 1). To control for batch effects between the two  
190 rounds of response phases (i.e., the immediate response treatment in December 2020 and the two  
191 delayed response treatments in June 2021), during each round we grew 10 replicate individuals  
192 of each species with sterilized potting mix (i.e., batch effect controls with no inoculum). In total,  
193 the response phase of our experiment included 660 pots (i.e., 180 pots for the immediate response  
194 treatment + 360 pots for the two delayed response treatments + 3 plant species  $\times$  10 replicates  $\times$  2  
195 rounds of field reference soil treatments + 3 plant species  $\times$  10 replicates  $\times$  2 rounds of batch effect



196 controls). We grew the plants in a growth chamber for 80 days (same conditions as the condition-  
197 ing phase, rotated weekly), after which we harvested, dried (72 hours at 60°C), and weighed plant  
198 aboveground biomass. At the end of all response phases, we collected soil samples from each pot  
199 to characterize the soil microbial community.

## 200 **DNA sequencing of the microbial community**

201 As described earlier, we collected soil samples from conditioned monoculture pots (before using  
202 them as soil inoculum) as well as response phase pots at the end of the experiment. The former was  
203 meant to characterize how seasonal time lag and plant litter affected the soil microbial community,  
204 while the latter was meant to see if these changes in the inoculum triggered long-lasting impacts  
205 (Hannula *et al.*, 2021). We mixed soils within each pot well and subsampled 0.25 g of soil. To  
206 each sample, we added 8 ng of P and F synthetic chimeric DNA spike for the quantification  
207 of prokaryotic and fungal absolute abundance prior to DNA extraction (Tkacz *et al.*, 2018). We  
208 extracted DNA using Qiagen DNeasy PowerSoil Pro Kit according to the manufacturer's manual,  
209 with a 65°C water bath incubation (10 minutes) prior to bead-beating to improve yield. Using two-  
210 step PCR, we amplified the V4 region of bacterial 16S ribosomal RNA gene (Caporaso *et al.*, 2012)  
211 and fungal internal spacer 1 region (ITS1) (White *et al.*, 1990) with index primers. We purified,  
212 normalized, and pooled amplicon libraries and sequenced using 2 × 300 bp paired-end Illumina  
213 MiSeq (see Supporting Methods S1).

## 214 **Data analysis**

### 215 *Microbial community*

216 We converted raw binary base call (BCL) files to fastq files and demultiplexed with Illumina  
217 Bcl2fastq2 (v2.20). We trimmed adapter sequences from reads using cutadapt (Martin, 2011) with  
218 python (v3.10.9). Using the Divisive Amplicon Denoising Algorithm (dada2 v.1.28.0) in R (v4.3.0),  
219 we quality filtered and trimmed the fastq files, and inferred amplicon sequence variants (ASV)  
220 (Callahan *et al.*, 2016a) following the published workflow (Callahan *et al.*, 2016b). Specifically, we  
221 discarded low-quality ends of reads by trimming the bacterial forward reads to 250 bp and the  
222 reverse reads to 210 bp, discarding any reads shorter than these lengths. We chose not to trim

223 fungal read lengths due to the varying size of the ITS gene region. We used phyloseq (McMurdie  
224 & Holmes, 2013) for downstream analysis. We discarded any ASV that was only detected in  $\leq 5$   
225 samples; we also removed samples with extremely small or large read counts (i.e., more or less  
226 than 5x the average number of reads across all samples). We rarefied samples to 5000 sequencing  
227 reads for downstream analyses.

228 We transformed the community matrix from raw reads to relative abundance. We calculated  
229 absolute abundance as in Tkacz *et al.* (2018). Briefly, we divided the total number of environmental  
230 reads by the number of synthetic reads in each sample and then multiplied it by the number of  
231 gene copies in the 8 ng of synthetic spike-in, which was calculated by multiplying the number  
232 of gene copies in 1 ng of spike-in (i.e.,  $3.5E+07$  for 16S and  $1.2E+07$  for ITS, respectively) by  
233 eight. To understand the starting soil microbial species pool that plants experience in the response  
234 phase, we explored differences in absolute abundances of 16s and ITS ASVs of the conditioned  
235 soil (immediately after the conditioning phase, after the six-month delay without litter, after the  
236 six-month delay with litter, and field reference soil). We first agglomerated the sequences in  
237 the conditioned soil samples to the class taxonomic level using `tax_glom` phyloseq function, and  
238 then visualized the total count for each class present in the samples. We identified compositional  
239 differences (i.e., beta diversity) with the Bray-Curtis dissimilarity metric and compared with a  
240 permutational multivariate analysis of variance using the `vegan` (Oksanen *et al.*, 2017) and `stats R`  
241 packages.

#### 242 *Plant biomass performance and competitive outcomes*

243 To test for differences in plant biomass when grown with conspecific-conditioned versus reference  
244 soil (i.e., unconditioned field soil and sterilized potting mix) microbes, we conducted a series  
245 of linear models with log-transformed biomass values as the response variable, and soil source  
246 as the predictor. We fit separate models per species (ACWR, FEMI, and PLER) and treatment  
247 (immediate, delayed with litter, delayed without litter) to facilitate model interpretation. Prior to  
248 biomass analyses, we filtered out outliers within each experiment phase  $\times$  species  $\times$  soil  $\times$  plant  
249 combination. Outliers were identified as individuals with biomass lower than  $Q1 - 1.5 * IQR$  or higher  
250 than  $Q3 + 1.5 * IQR$ , where  $Q1$  and  $Q3$  were the 25th or 75th quartiles, respectively, and  $IQR$  represents  
251 the difference between  $Q1$  and  $Q3$ . We evaluated statistical significance at  $\alpha = 0.05$ .

252 To predict how different response treatments modified the effects of plant–soil feedback on  
253 plant coexistence, we calculated microbially mediated stabilization and fitness differences for each  
254 treatment separately. We first quantified the effects of plant  $j$ -conditioned microbial community  
255 on the biomass performance of plant  $i$ , denoted as  $m_{ij}$  ( $i$  and  $j = 1$  or  $2$ ). This microbial effect is  
256 defined as  $m_{ij} = \ln(\text{biomass of plant } i \text{ in soil } j) - \ln(\text{biomass of plant } i \text{ in reference soil})$ , i.e., the  
257 rate of plant  $i$  biomass accumulation when grown in soils with the plant  $j$  microbial community  
258 relative to that in an unconditioned reference soil. We then compare pots with conspecific versus  
259 heterospecific soil inoculum to calculate microbially mediated stabilization and fitness differences  
260 following the theoretical derivations in Kandlikar *et al.* (2019) (see also Kandlikar *et al.*, 2021, Yan  
*et al.*, 2022):

$$\text{Stabilization} = -\frac{1}{2}(m_{11} - m_{12} - m_{21} + m_{22}) = \left(\frac{m_{21} + m_{12}}{2}\right) - \left(\frac{m_{11} + m_{22}}{2}\right), \quad (1)$$

$$\text{Fitness difference} = \frac{1}{2}(m_{11} + m_{12} - m_{21} - m_{22}) = \left(\frac{m_{11} + m_{12}}{2}\right) - \left(\frac{m_{21} + m_{22}}{2}\right). \quad (2)$$

261 Here, microbially mediated stabilization (eqn. 1) quantifies how plants condition the soil to impact  
262 heterospecific relative to conspecific competitors. Positive values favor coexistence, as conditioned  
263 soils more negatively (or less positively) impact their hosts. Negative values (i.e., destabilization)  
264 indicate that conditioned soils more positively (or less negatively) impact host plants, and can  
265 drive priority effects. On the other hand, microbially mediated fitness difference quantifies how  
266 conditioned microbes disproportionately impact one plant species over the other: in the form of  
267 eqn. 2, a positive value indicates that plant 1 is favored by soil microbes because they benefit more  
268 from mutualistic microbes and/or suffer less from pathogenic microbes, and vice versa. We can  
269 thereby predict microbially mediated competitive outcomes based on these two metrics. If the  
270 absolute value of fitness difference overwhelms the absolute value of stabilization, then the plant  
271 with higher fitness will outcompete the other plant (i.e., plant 1 wins if eqn. 2  $> 0$  while plant 2  
272 wins if eqn. 2  $< 0$ ). However, if the absolute value of stabilization exceeds that of fitness difference,  
273 then the theory predicts coexistence if eqn. 1  $> 0$  and priority effects if eqn. 1  $< 0$ . Comparing  
274 eqns 1 and 2 across the three response treatments allows us to evaluate our hypothesis regarding  
275 how seasonal time lag and litter decomposition alter the coexistence consequences of plant–soil  
276 feedback.

277 As an alternative predictor of coexistence, we also calculated the invasion growth rate (IGR)  
278 of each species within a competing species pair. Specifically, the IGR of species 1 when growing  
279 in the monoculture equilibrium of plant 2 and its corresponding soil microbe, and vice versa, are  
as follows (Kandlikar *et al.*, 2019):

$$\text{IGR}_1 = m_{12} - m_{22}, \quad (3)$$

$$\text{IGR}_2 = m_{21} - m_{11}. \quad (4)$$

280 If the two IGRs differ in their signs, then the species with a positive IGR will outcompete the  
281 species with a negative IGR. If both IGRs are positive (i.e., eqns 3 and 4 > 0), the two species  
282 are predicted to coexist as both can recover from low density; alternatively, the theory predicts  
283 priority effects if both IGRs are negative (i.e., eqns 3 and 4 < 0). Furthermore, each species' IGR  
284 only depends on how the resident soil microbe impacts the invader (e.g.,  $m_{12}$ ), relative to their  
285 impact on the resident host (e.g.,  $m_{22}$ ). Therefore, compared to eqns 1 and 2, which are aggregated  
286 metrics that incorporate the effects of both conditioned soil communities, it is easier to identify  
287 the key microbial impacts that are driving the changes in competitive outcome across response  
288 treatments.

289 We used a sampling approach to propagate the uncertainty when estimating  $m_{ij}$  through  
290 to the predictions of plant competitive outcome (Yan *et al.*, 2022, Terry & Armitage, 2023). Based  
291 on eqns 1–4, six different biomass terms are needed to predict the competitive outcome (i.e., the  
292 biomass of each plant species growing in soil 1, 2, and in the reference soil). For each sample draw,  
293 we randomly sampled one value for each of the six biomass terms from a normal distribution,  
294 with a mean equal to the empirical mean biomass and a standard deviation equal to the empirical  
295 standard error (SE). We repeated this procedure 1000 times for each species pair and calculated  
296 the stabilization, fitness difference, and invasion growth rates. This approach, compared to the  
297 commonly used orthogonal error bars (e.g., Kandlikar *et al.*, 2021), better propagates uncertainty  
298 as it captures the interdependence between parameter estimations (Terry & Armitage, 2023). All  
299 analyses were conducted in R (v4.3.0) (R Core Team, 2021).

## 300 Results

### 301 Microbial community

302 We first present results of the microbial community in the soil inocula, which revealed that sea-  
303 sonal time lag and plant litter decomposition had a clear impact on bacterial and fungal abundance  
304 (Fig. 2). The bacterial abundance was highest when sequenced immediately following the con-  
305 ditioning phase (i.e., inoculum used for the immediate response treatment). However, for all  
306 three plant species, it decreased consistently after a six-month delay period (i.e., inoculum used  
307 for the two delayed treatments; (Fig. 2A). The fungal community, while of much lower absolute  
308 abundance, showed the opposite trend where total abundance increased after the six-month de-  
309 lay period compared to that immediately after soil conditioning (Fig. 2B). The exception to this  
310 trend was soil conditioned by *F. microstachys* without the litter intact during the delay, where no  
311 fungal reads aside from the synthetic spike-in emerged after filtering. These results suggest that  
312 the responding seedlings interacted with different microbial communities in the three response  
313 treatments, due to the differences in microbial species pool in the soil inocula.

314 To evaluate whether different soil inocula led to divergent microbial composition, we also  
315 sequenced the microbial community at the end of each response phase (Fig. 3). As absolute  
316 abundances were quantified, we combined bacterial and fungal communities when analyzing  
317 differences in microbial community composition. For all soil sources conditioned by different  
318 plant species, microbial composition varied between response treatments (*A. wrangelianus*:  $R^2 =$   
319  $0.211$ ; *F. microstachys*:  $R^2 = 0.223$ ; *P. erecta*:  $R^2 = 0.210$ ; Reference soil:  $R^2 = 0.133$ ; all  $P < 0.05$ ). The  
320 response treatment was still the significant predictor for all soil inocula when the bacterial and  
321 fungal communities were analyzed separately (Fig. S1–S2).

### 322 Plant biomass

323 In the immediate response phase treatment, each of our focal species had lower aboveground  
324 biomass when grown with conspecific-conditioned soil microbes, relative to their growth in un-  
325 conditioned field microbial community (ACWR:  $F_{1,17} = 4.89$ ,  $P = 0.041$ ; FEMI:  $F_{1,16} = 10.64$ ,  $P =$   
326  $0.049$ ; PLER:  $F_{1,17} = 30.68$ ,  $P < 0.001$ ; Fig. 4; see also Fig. S3 for all biomass results). *F. microstachys*

327 and *P. erecta* grew worse in soils with a conspecific soil community than in sterilized potting mix  
328 (FEMI:  $F_{1,16} = 7.21, P = 0.016$ ; PLER:  $F_{1,16} = 9.53, P = 0.007$ ), while the opposite was true for  
329 *A. wrangelianus* ( $F_{1,16} = 4.53, P = 0.048$ ). Plants generally grew poorer in both delayed treat-  
330 ments (i.e., with/without litter present in conditioned soils during the time lag) compared to the  
331 immediate treatment (Fig. 4). Specifically, in the delayed treatments, *A. wrangelianus* grew substan-  
332 tially better when inoculated with any live soil microbial community than with sterilized potting  
333 mix, but its growth in conspecific-conditioned microbes was not significantly different than with  
334 an unconditioned field community (Fig. 4A). In contrast, *F. microstachys* growth in the delayed  
335 treatments was substantially lower with any live soil community than in sterilized potting mix.  
336 When litter was removed at the end of plant conditioning, conspecific-conditioned soil microbes  
337 resulted in lower plant biomass relative to unconditioned field microbes in *F. microstachys* and *P.*  
338 *erecta* (FEMI:  $F_{1,14} = 6.47, P = 0.02$ ; PLER:  $F_{1,18} = 27.57, P < 0.001$ ). This effect was diminished  
339 when plant litter was left intact after the soil conditioning phase.

#### 340 **Plant coexistence outcomes**

341 The aforementioned biomass differences across the three response treatments resulted in shifts in  
342 competitive outcomes for all three species pairs (Fig. 5). Although each species pair responded  
343 differently, the two delayed treatments mostly decreased the strength of stabilization (i.e., destabi-  
344 lization), with the exception being the delayed without litter treatment for the *A. wrangelianus*-*P.*  
345 *erecta* pair (Fig. 5C). The legume plant *A. wrangelianus* was predicted to outcompete *F. microstachys*  
346 and *P. erecta* in the immediate response treatment (green points in Fig. 5B-C). However, fitness  
347 differences shifted toward a direction that disfavor *A. wrangelianus* in the two delayed treatments  
348 (grey and brown points in Fig. 5B-C). Correspondingly, the IGR of *A. wrangelianus* became negative  
349 (Fig. 5E-F). As a result, *A. wrangelianus* loses its competitive dominance, exhibiting priority effect  
350 with *P. erecta* and being outcompeted by *F. microstachys* in the delayed with litter treatment.

351 We can also examine each species pair in more detail. For *F. microstachys* and *P. erecta*, the  
352 most common competitive outcome shifted from coexistence in the immediate treatment to *F.*  
353 *microstachys* outcompeting *P. erecta* in the delayed with litter treatment (Fig. 5A). In addition to  
354 destabilization, this shift in competitive outcome resulted from an increase in fitness difference in

355 favor of *F. microstachys*. The corresponding decrease in the IGR of *P. erecta* (Fig. 5D) indicates that the  
356 shift in competitive outcome was mainly driven by changes in the soil microbes conditioned by *F.*  
357 *microstachys*. For *A. wrangelianus* and *F. microstachys*, the most common competitive outcome shifted  
358 from *A. wrangelianus* dominance in the immediate treatment to *F. microstachys* dominance in the  
359 two delayed treatments (Fig. 5B). This change in competitive outcome mostly resulted from the flip  
360 in the competitive hierarchy between the two plants (i.e., a decrease in fitness difference in favor of  
361 *F. microstachys*). A corresponding flip in the sign of the two species' IGR can also be seen in Fig. 5E.  
362 For *A. wrangelianus* and *P. erecta*, the dominance of *A. wrangelianus* is the most common competitive  
363 outcome in the immediate treatment (Fig. 5C and E). The pair shifted towards coexistence (i.e., both  
364 plants have positive IGR) in the delayed treatment, but destabilization strengthened and resulted  
365 in priority effect (i.e., both plants have negative IGR) in the delayed with litter treatment.

## 366 Discussion

367 Typical two-phase plant–soil feedback greenhouse experiments grow the responding plant im-  
368 mediately after soil conditioning in the greenhouse (Brinkman *et al.*, 2010). When transplanted  
369 immediately, the predicted effects of soil microbes on species coexistence were consistent with  
370 those of a previous study using the same system — the legume *A. wrangelianus* benefited from  
371 microbially mediated fitness advantage and was predicted to outcompete the other two species  
372 (Kandlikar *et al.*, 2021) (light green points in Fig. 5). Yet during naturally occurring time lags of  
373 discrete growing seasons, the microbial community originally conditioned by plants may shift  
374 due to stochastic drift or biotic interactions between microbes. Moreover, the presence of litter can  
375 introduce microbes from other plant parts into the soil (Whitaker *et al.*, 2017, Fanin *et al.*, 2021) and  
376 the decomposition of litter can change the soil abiotic environment, thereby altering the soil micro-  
377 bial community (Veen *et al.*, 2021, Minás *et al.*, 2021). Thus, the microbial community encountered  
378 by a responding plant after the time delay may no longer resemble that of the original conditioning  
379 (Fig. 2). By quantifying stabilization and fitness differences, we show that microbially mediated  
380 plant coexistence outcomes change with the presence of a temporal delay and litter decomposition  
381 (grey and brown points in Fig. 5). Our study is a reminder that natural history, particularly in  
382 the form of temporal lags between consecutive generations, should be considered when designing



383 and inferring long-term coexistence from plant–soil feedback experiments.

384 Our sequencing results showed an increase in fungal abundance but a decrease in bacterial  
385 abundance between the initial conditioning phase and delayed phases (Fig.2). For both bacterial  
386 and fungal communities, the field reference soil contained the highest abundance of microbes. This  
387 is in line with the expectation that the field soil acts as a microbial species pool, which is thinned out  
388 to a smaller species-specific subset after plant conditioning. However, the high bacterial abundance  
389 in *A. wrangelianus* soil suggests that plants can also enrich specific microbes (Fig.2A). We speculate  
390 that the initial low abundance of fungi could be attributed to their slower growth rates, while the  
391 enrichment of saprotrophic Ascomycota fungi in the litter addition treatments results from their  
392 greater ability to utilize plant litter (Challacombe *et al.*, 2019). On the other hand, the decrease in  
393 bacterial abundance after the six-month delay could be attributed to drought-induced physiological  
394 stress, the lack of dormancy ability, and intensified resource competition with fungi (Shade *et al.*,  
395 2012, Schimel, 2018, Lennon *et al.*, 2021). When comparing the microbial community at the end of  
396 the response phases, we found that the total fungal and bacterial community diverges depending  
397 on response treatments (Fig. 3). This suggests that the temporal delay of previously conditioned  
398 soil will have a long-lasting impact on the microbial species pool and their corresponding impact  
399 during the next generation.

400 Our results are the first to demonstrate the influence of a temporal delay by leveraging recent  
401 advancements in plant–soil feedback theory (Kandlikar *et al.*, 2019). Moreover, our results highlight  
402 nuances when adopting modern coexistence theory to interpret empirical results. First, we show  
403 that quantifying invasion growth rates, in addition to the more commonly used stabilization and  
404 fitness difference metrics, yields a more nuanced understanding of the mechanisms through which  
405 microbial effects on plant coexistence arise. One example is the competition between *F. microstachys*  
406 and *P. erecta*, where the shift in competitive outcomes in the delayed treatments is caused by a loss  
407 of stabilization and an increase in fitness difference favoring *F. microstachys* (Fig. 5A). Examining  
408 the invasion growth rates suggests that the shift was primarily due to a decrease in the invasion  
409 growth rate of *P. erecta* (Fig. 5D), signifying a change in the microbial effects imposed by the soils of  
410 *F. microstachys*. Further investigation of plant biomass responses suggests that the observed shifts  
411 in coexistence outcomes arise because conditioned soils of *F. microstachys* substantially decrease

412 conspecific growth (relative to unconditioned reference) in the immediate treatment, but this  
413 negative impact of conditioned soils is minimal after the time lag (Fig. 4B). Second, instead of  
414 representing the uncertainty of stabilization and fitness difference as orthogonal error bars, we  
415 visualized the distribution of random samples (i.e., using the same approach as in Yan *et al.*, 2022  
416 but without the summary pie chart). Our results show that visualizing the spread of predicted  
417 outcomes reveals informative patterns: for example, in the case of *A. wrangelianus* and *P. erecta*,  
418 the diagonal distribution in the delayed-with-litter treatment arises due to the larger variation in  
419 the impact imposed by *P. erecta* soils (Ke & Wan, 2020). We echo recent calls for more careful  
420 considerations when calculating and visually presenting the uncertainty of predicted competitive  
421 outcomes (Terry & Armitage, 2023).

422 We incorporated litter dynamics in our experiment by preserving dead plant individuals  
423 in the pot during the temporal gap between the conditioning and response phases. This design  
424 corresponds well with our annual plant system, where litter input comes from natural plant senes-  
425 cence after the growing season. In other systems, different modes of plant death can generate  
426 litter dynamics that shape soil microbial communities differently. For instance, wind disturbances  
427 that uproot entire plants generate a substantial pulsed input of litter, potentially benefiting sapro-  
428 trophic microbes but adversely affecting obligated root-associated microbes (Cowden & Peterson,  
429 2013, Nagendra & Peterson, 2016). Conversely, herbivores and anthropogenic activities (e.g., clear-  
430 cutting) primarily remove aboveground parts while leaving belowground components intact in  
431 the soil. Such dynamics result in less aboveground litter, yet the remaining root tissues may con-  
432 tinue to support arbuscular mycorrhizal fungi (Pepe *et al.*, 2018). Recent studies have highlighted  
433 that aboveground and belowground litter differentially impact plant–soil microbe interactions.  
434 For example, Aldorfová *et al.* (2022) showed that root litter negatively affected plant performance  
435 due to enhanced pathogen transmission while shoot litter modified soil nutrient levels without  
436 significantly affecting plant growth. This complicated interplay between different belowground  
437 processes underscores the importance of including litter dynamics in microbially mediated plant–  
438 soil feedback studies (Ke *et al.*, 2015, Veen *et al.*, 2019).

439 We speculate that the impact of a temporal delay extends beyond that shown in our experi-  
440 ment. First, while we measured plant biomass performance following common plant-soil feedback

441 studies, the temporal delay may modify microbial effects on other plant demographic rates. For  
442 example, seed survival and germination of Californian annuals take place in dry soil after the  
443 Mediterranean summer. Following recent calls for studying microbial impact beyond biomass,  
444 we encourage future research to study the impact of microbial persistence on the early-stage seed-  
445 to-seedling transition (Dudenhöffer *et al.*, 2018, Miller *et al.*, 2019, Krishnadas & Stump, 2021).  
446 Furthermore, how persistent conditioned microbial effects are after plant death is an important  
447 question for many systems, not limited to systems with strong seasonality and non-overlapping  
448 generations. For instance, in systems with sparse vegetation cover (e.g., foredunes), a conditioned  
449 patch may be left vacant for extended periods due to dispersal limitation. In more complex systems  
450 with vertical structures (e.g., forests), one may argue that soil microbes mostly impact seedling  
451 survival on conditioned soil beneath the canopy of a living adult. However, the persistence of  
452 microbial effects following adult death and canopy opening can influence the performance of  
453 seedlings, thereby determining which species can successfully reach the canopy. Therefore, in-  
454 vestigating the persistence of conditioned microbial effects is likely more critical to community  
455 dynamics than previously recognized (Ke & Levine, 2021).

## 456 **Conclusion**

457 In our effort to bridge the gap between greenhouse experiments and natural ecosystems, we  
458 demonstrate the feasibility and importance of adjusting experimental schedules to provide a more  
459 realistic representation of natural systems. In light of our findings, we propose that in annual  
460 plant systems with non-overlapping generations, the intricate interplay of natural seasonality and  
461 litter dynamics prevent the direct extrapolation of plant–soil microbe interactions from one grow-  
462 ing season to the next. Our results reveal that the modification of plant–soil feedback following  
463 plant death is complex and varies between species pairs, thereby hindering generalizations based  
464 on studies that did not consider these factors. With the ongoing shifts in plant phenology and  
465 seasonal patterns due to climate change (Rudgers *et al.*, 2020), predicting plant community dynam-  
466 ics requires the explicit incorporation of the temporal aspects and natural history elements into  
467 plant–soil feedback research (Ke *et al.*, 2021).

## 468 **Acknowledgements**

469 We acknowledge the Chumash peoples as the traditional land caretakers where the soils and plants  
470 for this project were collected. We recognize that Stanford University occupies the ancestral land  
471 of native peoples in the Bay Area. This work was performed (in part) at the University of California  
472 Natural Reserve System (Sedgwick Reserve, Reserve DOI: 10.21973/N3C08R), under Application  
473 #45441. We thank Kate McCurdy and the staff of Sedgwick Reserve, the Kraft lab at UCLA for  
474 providing seeds, and Jonathan Levine for his feedback on the experimental design. This research  
475 was supported by the California Native Grasslands Association. PJK is supported by the Taiwan  
476 MOE Yushan scholar program (112V1010-3) and Taiwan NSCT (111-2621-B-002-001-MY3). MLW  
477 is supported by the USA NSF Graduate Research Fellowship (NSF GRFP DGE 1656518).

## 478 **Authorship Contribution**

479 SXO, GSK, and PJK conceptualized and designed the study. SXO performed the experiment and  
480 sample processing. All authors contributed to data analyses and writing.

## 481 **Data Availability Statement**

482 All primary data and computer scripts will be deposited on Github and Dryad upon submission.

483

## 484 References

- 485 **Aldorfová A, Dostálek T , Münzbergová Z. 2022.** Effects of soil conditioning, root and shoot litter  
486 addition interact to determine the intensity of plant–soil feedback. *Oikos*, **2022**: e09025.
- 487 **Barnard RL, Osborne CA , Firestone MK. 2013.** Responses of soil bacterial and fungal communities  
488 to extreme desiccation and rewetting. *The ISME Journal*, **7**: 2229–2241.
- 489 **Beals KK, Moore JA, Kivlin SN, Bayliss SL, Lumibao CY, Moorhead LC, Patel M, Summers JL,**  
490 **Ware IM, Bailey JK et al. 2020.** Predicting plant–soil feedback in the field: Meta-analysis reveals  
491 that competition and environmental stress differentially influence psf. *Frontiers in Ecology and*  
492 *Evolution*, **8**: 191.
- 493 **Beckman NG, Dybzinski R , Tilman D. 2022.** Short-term plant–soil feedback experiment fails to  
494 predict outcome of competition observed in long-term field experiment. *Ecology*, **104**: e3883.
- 495 **Bever JD, Dickie IA, Facelli E, Facelli JM, Klironomos J, Moora M, Rillig MC, Stock WD, Tibbett**  
496 **M, Zobel M. 2010.** Rooting theories of plant community ecology in microbial interactions. *Trends*  
497 *in Ecology & Evolution*, **25**: 468–478.
- 498 **Bever JD, Platt TG , Morton ER. 2012.** Microbial population and community dynamics on plant  
499 roots and their feedbacks on plant communities. *Annual Review of Microbiology*, **66**: 265–283.
- 500 **Bever JD, Westover KM , Antonovics J. 1997.** Incorporating the soil community into plant popu-  
501 lation dynamics: The utility of the feedback approach. *Journal of Ecology*, **85**: 561–573.
- 502 **Bonanomi G, Esposito A , Mazzoleni S. 2012.** Plant–soil feedback in herbaceous species of  
503 mediterranean coastal dunes. *Biological Letters*, **49**: 35–44.
- 504 **Brinkman EP, van der Putten WH, Bakker Ej , Verhoeven KJF. 2010.** Plant–soil feedback: ex-  
505 perimental approaches, statistical analyses and ecological interpretations. *Journal of Ecology*, **98**:  
506 1063–1073.
- 507 **Callahan BJ, McMurdie PJ, Rosen MJ, Han AW, Johnson AJA , Holmes SP. 2016a.** DADA2:  
508 high-resolution sample inference from illumina amplicon data. *Nature methods*, **13**: 581–583.

- 509 **Callahan BJ, Sankaran K, Fukuyama JA, McMurdie PJ, Holmes SP. 2016b.** Bioconductor work-  
510 flow for microbiome data analysis: from raw reads to community analyses. *F1000Research*,  
511 **5**.
- 512 **Caporaso JG, Lauber CL, Walters WA, Berg-Lyons D, Huntley J, Fierer N, Owens SM, Betley**  
513 **J, Fraser L, Bauer M et al. 2012.** Ultra-high-throughput microbial community analysis on the  
514 Illumina HiSeq and MiSeq platforms. *The ISME Journal*, **6**: 1621–1624.
- 515 **Challacombe JF, Hesse CN, Bramer LM, McCue LA, Lipton M, Purvine S, Nicora C, Gallegos-**  
516 **Graves LV, Porrás-Alfaro A, Kuske CR. 2019.** Genomes and secretomes of ascomycota fungi  
517 reveal diverse functions in plant biomass decomposition and pathogenesis. *BMC genomics*, **20**:  
518 1–27.
- 519 **Chesson P. 2000.** Mechanisms of maintenance of species diversity. *Annual Review of Ecology and*  
520 *Systematics*, **31**: 343–366.
- 521 **Cowden CC, Peterson CJ. 2013.** Annual and seasonal dynamics of ectomycorrhizal fungi coloniz-  
522 ing white pine (*Pinus strobus*) seedlings following catastrophic windthrow in northern Georgia,  
523 USA. *Canadian Journal of Forest Research*, **43**: 215–223.
- 524 **Crawford KM, Bauer JT, Comita LS, Eppinga MB, Johnson DJ, Mangan SA, Queenborough SA,**  
525 **Strand AE, Suding KN, Umbanhowar J et al. 2019.** When and where plant–soil feedback may  
526 promote plant coexistence: a meta-analysis. *Ecology Letters*, **22**: 1274–1284.
- 527 **Dudenhöffer JH, Ebeling A, Klein AM, Wagg C. 2018.** Beyond biomass: Soil feedbacks are  
528 transient over plant life stages and alter fitness. *Journal of Ecology*, **106**: 230–241.
- 529 **Ehrlén J, Eriksson O. 2000.** Dispersal limitation and patch occupancy in forest herbs. *Ecology*, **81**:  
530 1667–1674.
- 531 **Elmendorf SC, Harrison SP. 2009.** Temporal variability and nestedness in California grassland  
532 species composition. *Ecology*, **90**: 1492–1497.
- 533 **Eppinga MB, Baudena M, Johnson DJ, Jiang J, Mack KML, Strand AE, Bever JD. 2018.** Frequency-  
534 dependent feedback constrains plant community coexistence. *Nature Ecology & Evolution*, **2**:  
535 1403–1407.

- 536 **Esch CM , Kobe RK. 2021.** Short-lived legacies of *Prunus serotina* plant–soil feedbacks. *Oecologia*,  
537 **196:** 529–538.
- 538 **Fanin N, Lin D, Freschet GT, Keiser AD, Augusto L, Wardle DA , Veen GF. 2021.** Home-field  
539 advantage of litter decomposition: from the phyllosphere to the soil. *New Phytologist*, **231:**  
540 1353–1358.
- 541 **Forero LE, Grenzer J, Heinze J, Schittko C , Kulmatiski A. 2019.** Greenhouse- and field-measured  
542 plant–soil feedbacks are not correlated. *Frontiers in Environmental Science*, **7:** 184.
- 543 **Grainger TN, Levine JM , Gilbert B. 2019.** The invasion criterion: a common currency for  
544 ecological research. *Trends in Ecology & Evolution*, **34:** 925–935.
- 545 **Gundale MJ , Kardol P. 2021.** Multi-dimensionality as a path forward in plant–soil feedback  
546 research. *Journal of Ecology*, **109:** 3446–3465.
- 547 **Hannula SE, Heinen R, Huberty M, Steinauer K, De Long JR, Jongen R , Bezemer TM. 2021.**  
548 Persistence of plant-mediated microbial soil legacy effects in soil and inside roots. *Nature Com-*  
549 *munications*, **12:** 5686.
- 550 **Kandlikar GS, Johnson CA, Yan X, Kraft NJ , Levine JM. 2019.** Winning and losing with microbes:  
551 how microbially mediated fitness differences influence plant diversity. *Ecology Letters*, **22:** 1178–  
552 1191.
- 553 **Kandlikar GS, Yan X, Levine JM , Kraft NJ. 2021.** Soil microbes generate stronger fitness differences  
554 than stabilization among california annual plants. *The American Naturalist*, **197:** E30–E39.
- 555 **Ke PJ , Levine JM. 2021.** The temporal dimension of plant–soil microbe interactions: mechanisms  
556 promoting feedback between generations. *The American Naturalist*, **198:** E80–E94.
- 557 **Ke PJ, Miki T , Ding T. 2015.** The soil microbial community predicts the importance of plant traits  
558 in plant–soil feedback. *New Phytologist*, **206:** 329–341.
- 559 **Ke PJ , Wan J. 2020.** Effects of soil microbes on plant competition: a perspective from modern  
560 coexistence theory. *Ecological Monographs*, **90:** e01391.



- 561 **Ke PJ , Wan J. 2023.** A general approach for quantifying microbial effects on plant competition.  
562 *Plant and Soil*, **485**: 57–70.
- 563 **Ke PJ, Zee PC , Fukami T. 2021.** Dynamic plant–soil microbe interactions: the neglected effect of  
564 soil conditioning time. *New Phytologist*, **231**: 1546–1558.
- 565 **Krishnadas M , Stump SM. 2021.** Dispersal limitation and weaker stabilizing mechanisms mediate  
566 loss of diversity with edge effects in forest fragments. *Journal of Ecology*, **109**: 2137–2151.
- 567 **Lennon JT, den Hollander F, Wilke-Berenguer M , Blath J. 2021.** Principles of seed banks and the  
568 emergence of complexity from dormancy. *Nature Communications*, **12**: 1–16.
- 569 **Martin M. 2011.** Cutadapt removes adapter sequences from high-throughput sequencing reads.  
570 *EMBnet. Journal*, **17**: 10–12.
- 571 **McMurdie PJ , Holmes S. 2013.** phyloseq: an R package for reproducible interactive analysis and  
572 graphics of microbiome census data. *PloS ONE*, **8**: e61217.
- 573 **Miller EC, Perron GG , Collins CD. 2019.** Plant-driven changes in soil microbial communities  
574 influence seed germination through negative feedbacks. *Ecology and Evolution*, **9**: 9298–9311.
- 575 **Miller ZR , Allesina S. 2021.** Metapopulations with habitat modification. *Proceedings of the National*  
576 *Academy of Sciences of the United States of America*, **118**: e2109896118.
- 577 **Minás A, García-Parisi PA, Chludil H , Omacini M. 2021.** Endophytes shape the legacy left by the  
578 above- and below-ground litter of the host affecting the establishment of a legume. *Functional*  
579 *Ecology*, **35**: 2870–2881.
- 580 **Nagendra UJ , Peterson CJ. 2016.** Plant–soil feedbacks differ in intact and tornado-damaged areas  
581 of the southern Appalachian mountains, USA. *Plant and Soil*, **402**: 103–116.
- 582 **Nilsson RH, Larsson KH, Taylor AFS, Bengtsson-Palme J, Jeppesen TS, Schigel D, Kennedy P,**  
583 **Picard K, Glöckner FO, Tedersoo L et al. 2019.** The unite database for molecular identification  
584 of fungi: handling dark taxa and parallel taxonomic classifications. *Nucleic Acids Research*, **47**:  
585 D259–D264.

- 586 **Oksanen J, Blanchet FG, Friendly M, Kindt R, Legendre P, McGlenn D, Minchin PR, O'Hara**  
587 **RB, Simpson GL, Solymos P et al.** 2017. *vegan: Community Ecology Package*. R package version  
588 2.4-2.
- 589 **Pepe A, Giovannetti M , Sbrana C.** 2018. Lifespan and functionality of mycorrhizal fungal  
590 mycelium are uncoupled from host plant lifespan. *Scientific Reports*, **8**: 1–10.
- 591 **Png GK, De Long JR, Fry EL, Heinen R, Heinze J, Morriën E, Sapsford SJ , Teste FP.** 2023.  
592 Plant-soil feedback: the next generation. *Plant and Soil*, **485**: 1–5.
- 593 **van der Putten WH, Bardgett RD, Bever JD, Bezemer TM, Casper BB, Fukami T, Kardol P,**  
594 **Klironomos JN, Kulmatiski A, Schweitzer JA et al.** 2013. Plant–soil feedbacks : the past, the  
595 present and future challenges. *Journal of Ecology*, **101**: 265–276.
- 596 **Quast C, Pruesse E, Yilmaz P, Gerken J, Schweer T, Yarza P, Peplies J , Glöckner FO.** 2012.  
597 The silva ribosomal rna gene database project: improved data processing and web-based tools.  
598 *Nucleic Acids Research*, **41**: D590–D596.
- 599 **R Core Team.** 2021. *R: A Language and Environment for Statistical Computing*. R Foundation for  
600 Statistical Computing, Vienna, Austria.
- 601 **Rudgers JA, Afkhami ME, Bell-Dereske L, Chung YA, Crawford KM, Kivlin SN, Mann MA ,**  
602 **Nuñez MA.** 2020. Climate disruption of plant–microbe interactions. *Annual Review of Ecology,*  
603 *Evolution, and Systematics*, **51**: 561–586.
- 604 **Schimel JP.** 2018. Life in dry soils: effects of drought on soil microbial communities and processes.  
605 *Annual Review of Ecology, Evolution, and Systematics*, **49**: 409–432.
- 606 **Shade A, Peter H, Allison SD, Baho D, Berga M, Bürgmann H, Huber DH, Langenheder S,**  
607 **Lennon JT, Martiny JB et al.** 2012. Fundamentals of microbial community resistance and  
608 resilience. *Frontiers in Microbiology*, **3**: 417.
- 609 **Siefert A, Zillig KW, Friesen ML , Strauss SY.** 2019. Mutualists stabilize the coexistence of  
610 congeneric legumes. *The American Naturalist*, **193**: 200–212.

- 611 **Terry CD , Armitage DW. 2023.** Widespread analytical pitfalls in empirical coexistence studies  
612 and a checklist for improving their statistical robustness. *bioRxiv*, pp. 2023–07.
- 613 **Tkacz A, Hortala M , Poole PS. 2018.** Absolute quantitation of microbiota abundance in environ-  
614 mental samples. *Microbiome*, **6**: 110.
- 615 **Turelli M. 1978.** A reexamination of stability in randomly varying versus deterministic envi-  
616 ronments with comments on the stochastic theory of limiting similarity. *Theoretical Population*  
617 *Biology*, **13**: 244–267.
- 618 **Veen C, Fry E, ten Hooven F, Kardol P, Morriën E , De Long JR. 2019.** The role of plant litter in  
619 driving plant–soil feedbacks. *Frontiers in Environmental Science*, **7**: 168.
- 620 **Veen GF, ten Hooven FC, Weser C , Hannula SE. 2021.** Steering the soil microbiome by repeated  
621 litter addition. *Journal of Ecology*, **109**: 2499–2513.
- 622 **Whitaker BK, Bauer JT, Bever JD , Clay K. 2017.** Negative plant-phylosphere feedbacks in native  
623 asteraceae hosts—a novel extension of the plant–soil feedback framework. *Ecology Letters*, **20**:  
624 1064–1073.
- 625 **White TJ, Bruns T, Lee S, Taylor J et al. 1990.** Amplification and direct sequencing of fungal  
626 ribosomal RNA genes for phylogenetics. *PCR protocols: a guide to methods and applications*, **18**:  
627 315–322.
- 628 **Yan X, Levine JM , Kandlikar GS. 2022.** A quantitative synthesis of soil microbial effects on plant  
629 species coexistence. *Proceedings of the National Academy of Sciences of the United States of America*,  
630 **119**: e2122088119.

## 631 **Figure legends**

632 **Figure 1.** Schematic diagram of the two-phase plant–soil feedback experiment with three fully  
633 factorial response treatments: the immediate transplant treatment (light green pots), the delayed  
634 without litter treatment (grey pots), and the delayed with litter treatment (brown pots). The two  
635 rounds of response phases are six months apart, each including a treatment with field uncondi-  
636 tioned soil as references (blue pots). Note that the sterilized soil treatments and batch control pots  
637 are not included in this illustration (see Methods).

638 **Figure 2.** Absolute abundance of (A) bacterial and (B) fungal taxa (aggregated at the Class level)  
639 within the soil inocula used for different response treatments. Each stacked bar represents the ab-  
640 solute abundance of microbial taxa (x-axis and colors) within a specific soil inoculum (y-axis). The  
641 inocula are differentiated by their conditioning host species (i.e., *Acmispon wrangelianus* (ACWR);  
642 *Festuca microstachys* (FEMI); *Plantago erecta* (PLER)) and response treatments (i.e., immediate re-  
643 sponse, delayed without litter, and delayed with litter). The top row, labeled as field reference,  
644 depicts soil samples collected from Sedgwick Reserve at the experiment’s outset (i.e., prior to the  
645 growth of any conditioning individual).

646 **Figure 3.** Principal coordinates analysis (PCoA) for the combined soil microbial community  
647 composition (i.e., bacterial 16S and fungal ITS) sequenced at the end of the response phase. Each  
648 panel represents a different inoculum source (conditioning host plant). From left to right: *Acmispon*  
649 *wrangelianus* (ACWR); *Festuca microstachys* (FEMI); *Plantago erecta* (PLER); unconditioned Sedgwick  
650 Reserve field soil as reference soil (REF). Each point represents the microbial community sampled  
651 from a seedling at the end of the response phase and the shape represents its species identity. Colors  
652 represent the three response treatments: immediate (light green), delayed without litter (grey),  
653 and delayed with litter (brown). As the two delayed treatments shared the same reference soil  
654 controls, we omitted one of the delayed treatment in the rightmost panel. Purple circles (labeled  
655 as SW) represent soils collected from Sedgwick Reserve at the beginning of the experiment (i.e.,  
656 without the growth of any conditioning or responding individual) and were added for visualization  
657 purposes.

658 **Figure 4.** Effects of soil microbial inocula on plant biomass for (A) *Acmispon wrangelianus* (ACWR),  
659 (B) *Festuca microstachys* (FEMI), and (C) *Plantago erecta* (PLER). Each panel shows the aboveground  
660 biomass (log-scale x-axis) of the focal plant, grown with a soil microbial community that had been  
661 conditioned by conspecifics (blue) or heterospecifics (grey circles); unconditioned communities  
662 from field soil (green); or sterilized potting mix (brown). Note that the two delayed treatments  
663 shared the same field reference and sterilized potting mix controls. The three plant-conditioned  
664 soil inocula are ordered (from bottom to top) as follows: ACWR, FEMI, and PLER. Larger symbols  
665 indicate the mean biomass, error bars show  $2 \times \text{SEM}$ , and small points show each individual  
666 biomass.

667 **Figure 5.** Predicted competitive outcomes between pairs of plants: (A & D) *Festuca microstachys*  
668 (FEMI) and *Plantago erecta* (PLER); (B & E) *Acmispon wrangelianus* (ACWR) and *F. microstachys*; (C &  
669 F) *A. wrangelianus* and *P. erecta*. For each panel, the first and second species listed on the facet label  
670 correspond to species 1 and 2 in eqns 1–4, respectively. (A–C) The parameter space of stabilization  
671 (x-axis) and fitness difference (y-axis) for the three species pairs. Each region represents different  
672 predicted competitive outcomes: the right and left grey triangular regions represent coexistence  
673 and priority effect, respectively. The upper and lower white triangular regions represent the  
674 dominance of species 1 and 2, respectively. For each species pair, the three response treatments  
675 are plotted on the same panel and are indicated by different colors: immediate (light green),  
676 delayed without litter (grey), and delayed with litter (brown). Each translucent point represents  
677 a random draw (see Methods) and the open black circle represents the mean stabilization and  
678 fitness difference of 1000 random draws. (D–E) Invasion growth rates (IGR, y-axis) for the three  
679 species pair under different response treatments (x-axis). Different colors represent different plant  
680 species: ACWR (green), FEMI (orange), and PLER (purple).

## 681 **Supporting Information**

682 The following Supporting Information is available for this article:

683 **Methods S1.** Supporting methods for soil microbial community characterization

684 **Fig. S1.** Principal coordinates analysis for the bacterial community composition

685 **Fig. S2.** Principal coordinates analysis for the fungal community composition

686 **Fig. S3.** Effects of soil microbial inocula on plant biomass in all response and control treatments

687 **Figures**

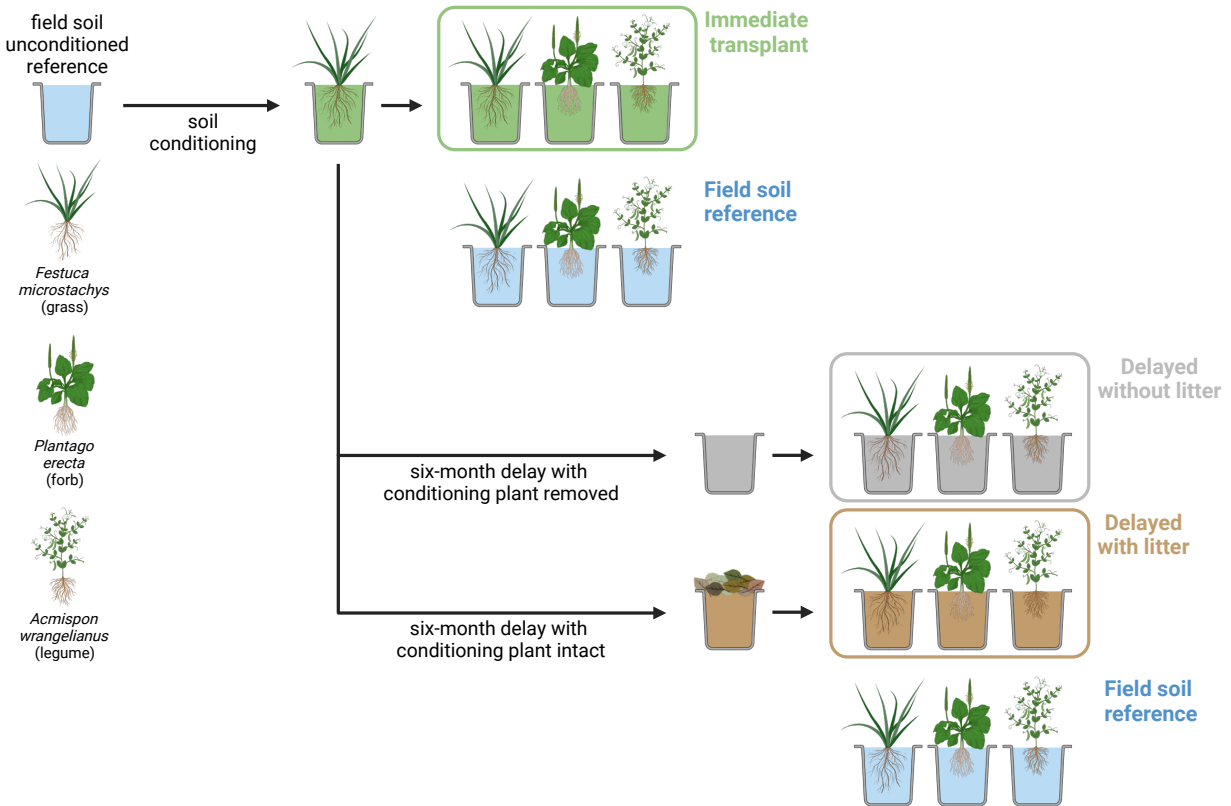


**Figure 1** Schematic diagram of the two-phase plant–soil feedback experiment with three fully factorial response treatments: the immediate transplant treatment (light green pots), the delayed without litter treatment (grey pots), and the delayed with litter treatment (brown pots). The two rounds of response phases are six months apart, each including a treatment with field unconditioned soil as references (blue pots). Note that the sterilized soil treatments and batch control pots are not included in this illustration (see Methods).



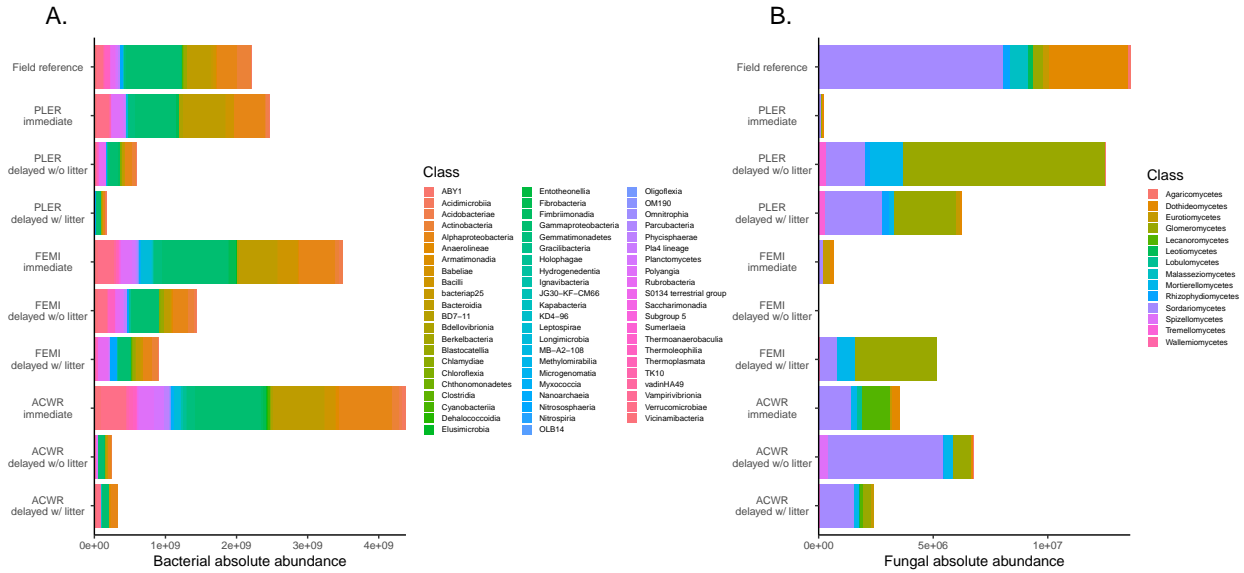


**Figure 2** Absolute abundance of (A) bacterial and (B) fungal taxa (aggregated at the Class level) within the soil inocula used for different response treatments. Each stacked bar represents the absolute abundance of microbial taxa (x-axis and colors) within a specific soil inoculum (y-axis). The inocula are differentiated by their conditioning host species (i.e., *Acmispon wrangelianus* (ACWR); *Festuca microstachys* (FEMI); *Plantago erecta* (PLER)) and response treatments (i.e., immediate response, delayed without litter, and delayed with litter). The top row, labeled as field reference, depicts soil samples collected from Sedgwick Reserve at the experiment's outset (i.e., prior to the growth of any conditioning individual).

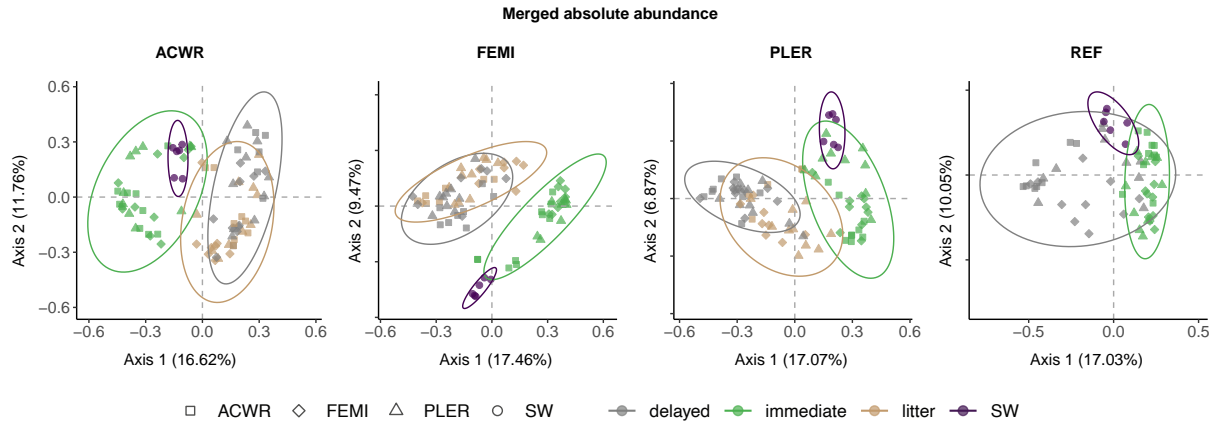


**Figure 3** Principal coordinates analysis (PCoA) for the combined soil microbial community composition (i.e., bacterial 16S and fungal ITS) sequenced at the end of the response phase. Each panel represents a different inoculum source (conditioning host plant). From left to right: *Acmispon wrangelianus* (ACWR); *Festuca microstachys* (FEMI); *Plantago erecta* (PLER); unconditioned Sedgwick Reserve field soil as reference soil (REF). Each point represents the microbial community sampled from a seedling at the end of the response phase and the shape represents its species identity. Colors represent the three response treatments: immediate (light green), delayed without litter (grey), and delayed with litter (brown). As the two delayed treatments shared the same reference soil controls, we omitted one of the delayed treatment in the rightmost panel. Purple circles (labeled as SW) represent soils collected from Sedgwick Reserve at the beginning of the experiment (i.e., without the growth of any conditioning or responding individual) and were added for visualization purposes.

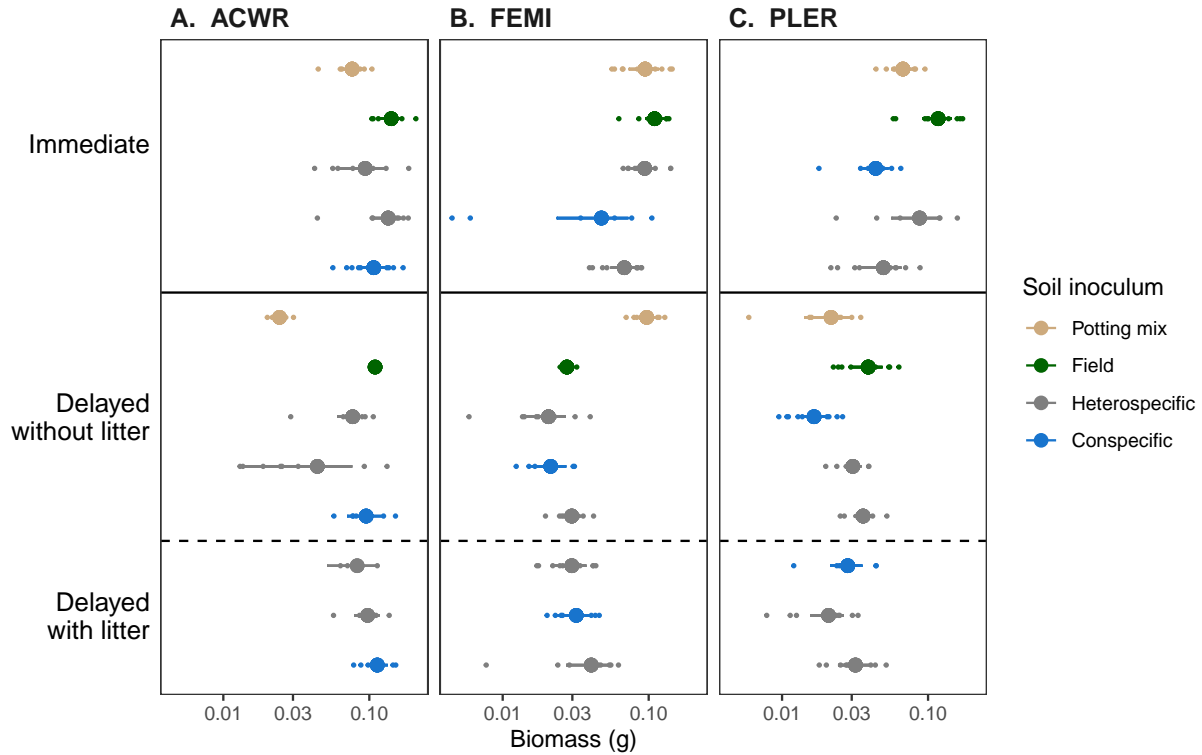


**Figure 4** Effects of soil microbial inocula on plant biomass for (A) *Acmispon wrangelianus* (ACWR), (B) *Festuca microstachys* (FEMI), and (C) *Plantago erecta* (PLER). Each panel shows the aboveground biomass (log-scale x-axis) of the focal plant, grown with a soil microbial community that had been conditioned by conspecifics (blue) or heterospecifics (grey circles); unconditioned communities from field soil (green); or sterilized potting mix (brown). Note that the two delayed treatments shared the same field reference and sterilized potting mix controls. The three plant-conditioned soil inocula are ordered (from bottom to top) as follows: ACWR, FEMI, and PLER. Larger symbols indicate the mean biomass, error bars show  $2 \times \text{SEM}$ , and small points show each individual biomass.

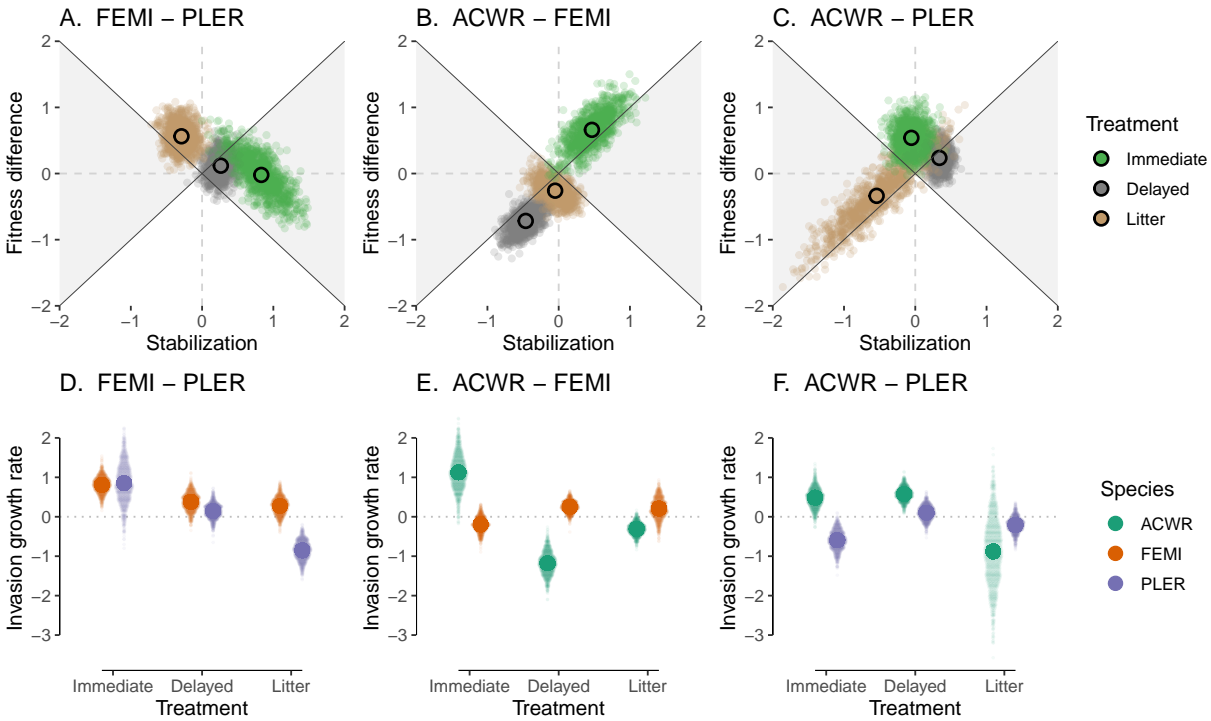


**Figure 5** Predicted competitive outcomes between pairs of plants: (A & D) *Festuca microstachys* (FEMI) and *Plantago erecta* (PLER); (B & E) *Acmispon wrangelianus* (ACWR) and *F. microstachys*; (C & F) *A. wrangelianus* and *P. erecta*. For each panel, the first and second species listed on the facet label correspond to species 1 and 2 in eqns 1–4, respectively. (A–C) The parameter space of stabilization (x-axis) and fitness difference (y-axis) for the three species pairs. Each region represents different predicted competitive outcomes: the right and left grey triangular regions represent coexistence and priority effect, respectively. The upper and lower white triangular regions represent the dominance of species 1 and 2, respectively. For each species pair, the three response treatments are plotted on the same panel and are indicated by different colors: immediate (light green), delayed without litter (grey), and delayed with litter (brown). Each translucent point represents a random draw (see Methods) and the open black circle represents the mean stabilization and fitness difference of 1000 random draws. (D–E) Invasion growth rates (IGR, y-axis) for the three species pair under different response treatments (x-axis). Different colors represent different plant species: ACWR (green), FEMI (orange), and PLER (purple).

## Supporting Information for

# Realistic time-lags and litter dynamics alter predictions of plant–soil feedback across generations

Suzanne X. Ou<sup>1</sup>, Gaurav S. Kandlikar<sup>2,3</sup>, Magdalena L. Warren<sup>1</sup>, and Po-Ju Ke<sup>4,†</sup>

<sup>1</sup>Department of Biology, Stanford University, Stanford, CA 94305, USA

<sup>2</sup>Department of Biological Sciences, Louisiana State University, Baton Rouge, LA 70803, USA

<sup>3</sup>Division of Biological Sciences, University of Missouri, Columbia, MO 65211, USA

<sup>4</sup>Institute of Ecology and Evolutionary Biology, National Taiwan University, Taipei, Taiwan

1

## 2 **Supporting Methods S1**

### 3 **Synthetic spike-in**

4 Using the synthetic spike-in method from Tkacz *et al.* (2018), we bought plasmids with p-Spike P  
5 for prokaryotic 16S (<https://www.addgene.org/101172/>) and p-Spike F for fungal communities  
6 (<https://www.addgene.org/101174/>). We plated the plasmids on Luria Broth (LB) media with  
7 carbenicillin for the ampicillin selection marker and incubated overnight in 25°C. We then picked a  
8 colony and inoculated 10 mL of LB broth containing carbenicillin and incubated at 30°C / 120rpm  
9 measuring CD on a nanodrop machine at 2 hour intervals until CD concentration = 1. Using  
10 zymoPURE Plasmid miniprep kit, we eluted plasmid DNA and measured DNA concentration  
11 using High Sensitivity dsDNA Qubit Assay (ThermoFisher, Waltham, MA). We loaded a subsample  
12 of the eluted plasmid DNA for gel electrophoresis to check for the correct plasmid size.

### 13 **Amplicon sequencing**

14 For bacterial metabarcoding, we amplified the highly variable (V4) region of the 16s rRNA gene  
15 using primers 515F (5'- TCG TCG GCA GCG TCA GAT GTG TAT AAG AGA CAG GTG YCA GCM

---

† Correspondence author: [pojuko@ntu.edu.tw](mailto:pojuko@ntu.edu.tw)

16 GCC GCG GTAA -3') and 806R (5'- GTC TCG TGG GCT CGG AGA TGT GTA TAA GAG ACA  
17 GGG ACT ACN VGG GTW TCT AAT -3'). For fungal metabarcoding, we amplified the fungal  
18 ITS1 region using primers based on the ITS1F (5'- AAT GAT ACG GCG ACC ACC GAG ATC TAC  
19 ACG GCT TGG TCA TTT AGA GGA AGT AA -3') and ITS2 (5'- CAA GCA GAA GAC GGC ATA  
20 CGA GAT - [INDEX] - CGG CTG CGT TCT TCA TCG ATGC -3'), where [INDEX] is a sample-  
21 specific 12-nt error-correcting Golay barcode. Illumina adapters on each 5' end of the primers were  
22 used to attach unique Nextera XT indexes for sample identification. First step PCR consisted of  
23 3.2 $\mu$ L of PCR-grade water, 5 $\mu$ L of Meridian Bioscience MyTaq HS Red Mix (Bioline, Tunton, MA),  
24 0.4 $\mu$ L each of forward and reverse primers, and 1 $\mu$ L of extracted DNA. PCR cycles were: 95°C  
25 for 2 min, 35 cycles of 95°C for 20 sec, 50°C for 20 sec, 72°C for 50 sec, and a final extension at  
26 72°C for 10 min with storage at 4°C. We confirmed amplification by gel electrophoresis. Second  
27 step PCR consisted of 3.2 $\mu$ L of PCR-grade water, 5 $\mu$ L of Meridian Bioscience MyTaq HS Red Mix  
28 (Bioline, Tunton, MA), 0.4 $\mu$ L each of Nextera XT index primers 1 and 2, and 1 $\mu$ L of first step PCR  
29 product. We confirmed amplification by gel electrophoresis and purified amplicons using Sera-  
30 Mag Speedbeads (Sigma-Aldrich, St. Louis, MO). We quantified DNA concentration using High  
31 Sensitivity dsDNA Qubit Assay (Thermofisher, Waltham, MA) and pooled evenly across samples  
32 to a concentration of 4nM. The final DNA concentration was quantified using BioAnalyzer and  
33 sequenced on an Illumina MiSeq sequencer (2 X 300 cycle sequencing kit, Illumina, San Diego, CA)  
34 with a 15% PhiX spike-in at the Stanford Genomic Sequencing Service Center.

## 35 **Metabarcoding analysis**

36 Reads were demultiplexed and assigned to samples using Illumina bcl2fastq conversion software.  
37 We processed ITS1 and 16S samples separately. We trimmed raw amplicon sequences using  
38 Cutadapt (Martin, 2011). We used the DADA2 pipeline (Callahan *et al.*, 2016a) to merge paired-end  
39 sequences, quality filter, remove chimeric reads, and cluster sequences into amplicon sequence  
40 variants (ASVs). We used the SILVA database (Quast *et al.*, 2012) for 16S taxonomic assignment and  
41 the UNITE database (Nilsson *et al.*, 2019) for ITS taxonomic assignment. We removed any ASV that  
42 was present in  $\leq 5$  samples or whose relative abundance was  $< 0.01$  across all samples. We also  
43 removed samples with extremely small or large read counts (i.e., more or less than 5x the average

44 number of reads across all samples). We rarefied samples to 5000 sequencing reads.



## 45 Supporting Figures

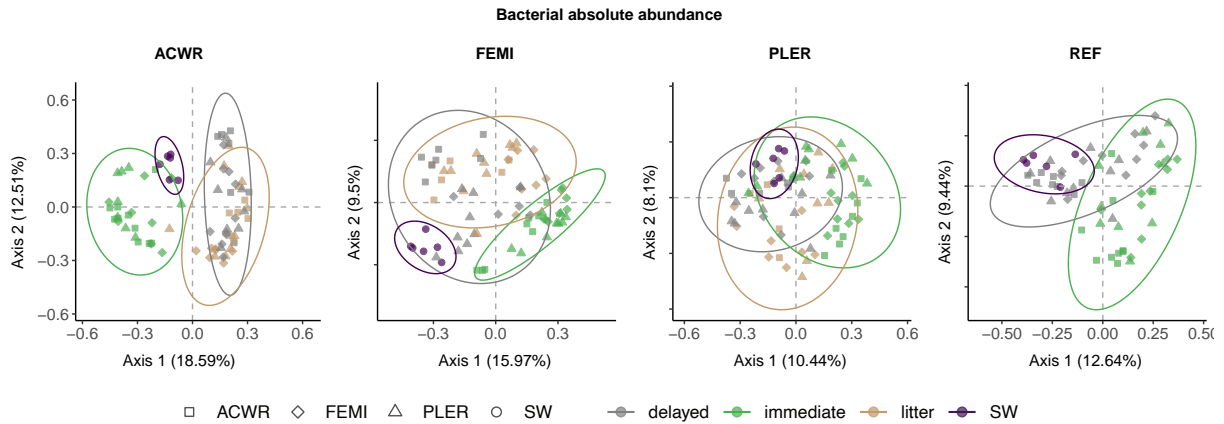


**Figure S1** Principal coordinates analysis (PCoA) for the bacterial community composition sequenced at the end of the response phase. Each panel represents a different inoculum source (conditioning host plant). From left to right: *Acmispon wrangelianus* (ACWR); *Festuca microstachys* (FEMI); *Plantago erecta* (PLER); unconditioned Sedgwick Reserve field soil as reference soil (REF). Each point represents the microbial community sampled from a seedling at the end of the response phase and the shape represents its species identity. Colors represent the three response treatments: immediate (light green), delayed without litter (grey), and delayed with litter (brown). As the two delayed treatments shared the same reference soil controls, we omitted one of the delayed treatment in the rightmost panel. Purple circles (labeled as SW) represent soils collected from Sedgwick Reserve at the beginning of the experiment (i.e., without the growth of any conditioning or responding individual) and were added for visualization purposes.

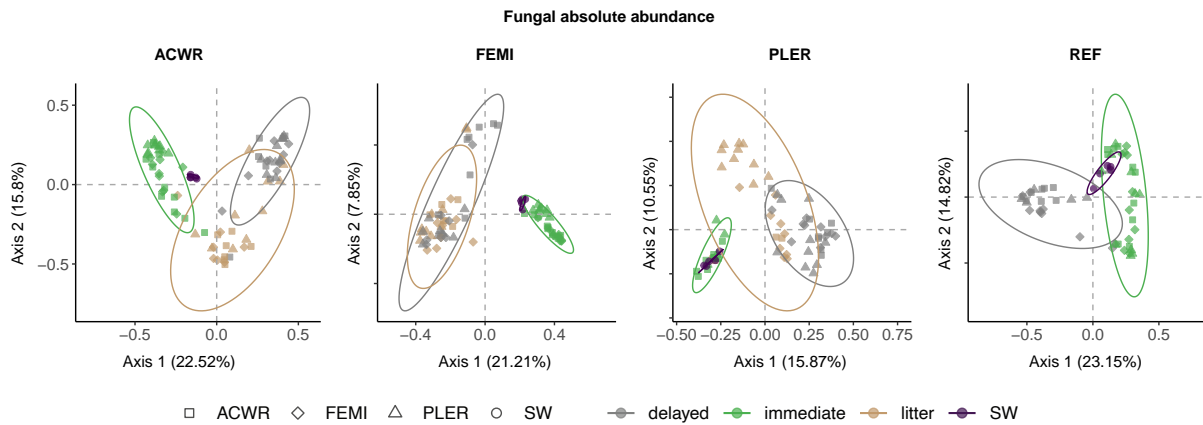


**Figure S2** Principal coordinates analysis (PCoA) for the fungal community composition sequenced at the end of the response phase. Each panel represents a different inoculum source (conditioning host plant). From left to right: *Acmispon wrangelianus* (ACWR); *Festuca microstachys* (FEMI); *Plantago erecta* (PLER); unconditioned Sedgwick Reserve field soil as reference soil (REF). Each point represents the microbial community sampled from a seedling at the end of the response phase and the shape represents its species identity. Colors represent the three response treatments: immediate (light green), delayed without litter (grey), and delayed with litter (grown). As the two delayed treatments shared the same reference soil controls, we omitted one of the delayed treatment in the rightmost panel. Purple circles (labeled as SW) represent soils collected from Sedgwick Reserve at the beginning of the experiment (i.e., without the growth of any conditioning or responding individual) and were added for visualization purposes.

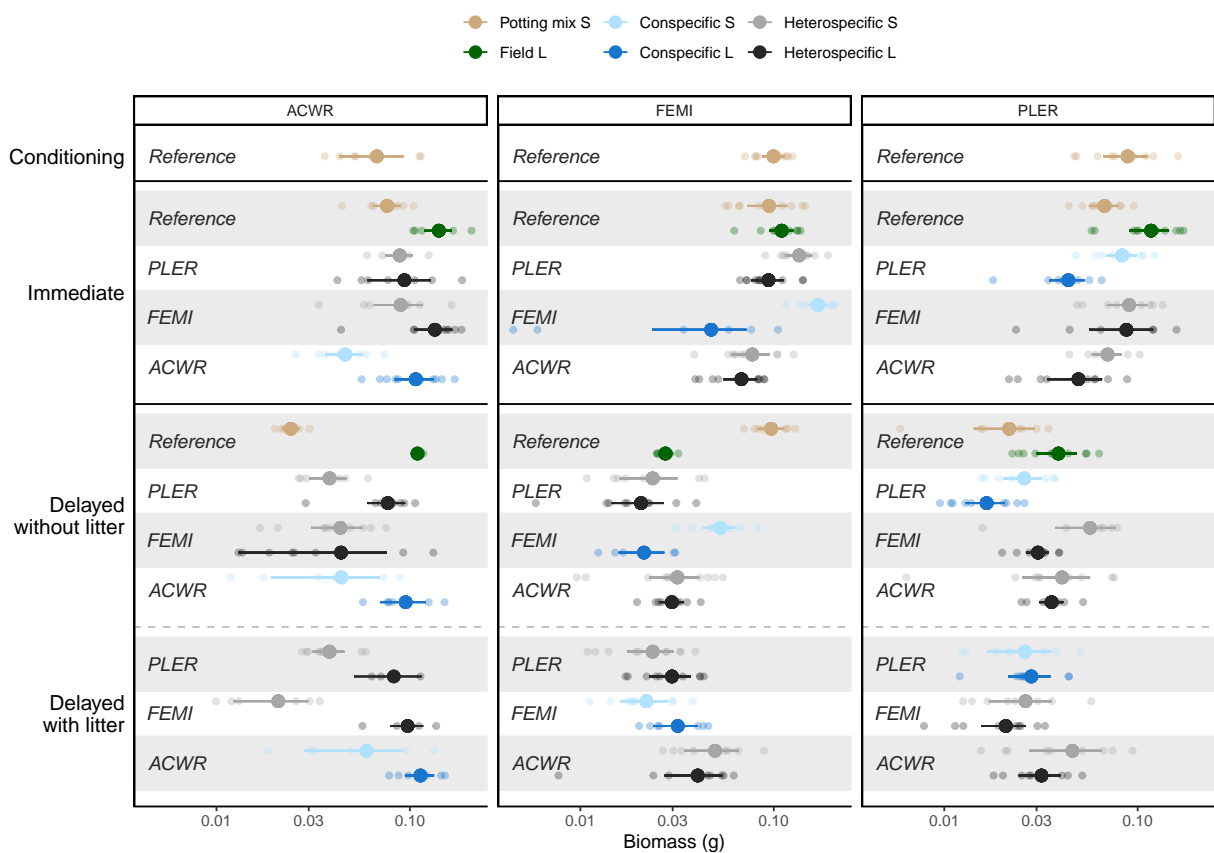


**Figure S3** Effects of soil microbial inocula on plant biomass in all response and control treatments for (A) *Acmispon wrangelianus* (ACWR), (B) *Festuca microstachys* (FEMI), and (C) *Plantago erecta* (PLER). Capital "S" indicates sterilized soils and "L" indicates live unsterilized soils. Colors represent different soil inocula: sterilized potting mix (brown), unconditioned field soil (green), soil conditioned by conspecifics (blue), soil conditioned by conspecifics but sterilized (light blue), soils conditioned by heterospecifics (dark grey), and soils conditioned by heterospecifics but sterilized (light grey). Note that the two delayed treatments shared the same field reference and sterilized potting mix controls. The three plant-conditioned soil inocula are ordered (from bottom to top) as follows: ACWR, FEMI, and PLER. Larger symbols indicate the mean biomass, error bars show  $2 \times \text{SEM}$ , and small points show each individual biomass.